RESEARCH   **Open Access**

Alteration of the gut microbiome in mycophenolate-induced enteropathy: impacts on the profile of short-chain fatty acids in a mouse model

Manon Jardou[1], Quentin Provost[1], Clarisse Brossier[1], Émilie Pinault[1], François-Ludovic Sauvage[1] and Roland Lawson[1,2]*

Abstract

Background: Mycophenolic acid (MPA) is the most widely used immunosuppressive drug in transplantation and for autoimmune diseases. Unfortunately, more than 30% of patients experience a typical gastrointestinal adverse effect also referred to as mycophenolate-induced enteropathy. Due to its antibacterial, antifungal, and antiviral properties, MPA exposure is associated with intestinal dysbiosis characterized by a decrease in density and diversity of the microbiome regarding the main bacterial phyla (Firmicutes and Bacteroidetes). These bacterial phyla are known for their metabolic role in maintaining the homeostasis of the digestive tract, particularly through the production of short-chain fatty acids (SCFA) that could contribute to the pathophysiology of mycophenolate-induced enteropathy. Our study aimed at deciphering short-chain fatty acids (SCFA) profile alterations associated with gastrointestinal toxicity of MPA at the digestive and systemic levels in a mouse model.

Methods: Ten-week old C57BL/6 (SOPF) mice were randomly assigned in 2 groups of 9 subjects: control, and mycophenolate mofetil (MMF, 900 mg/kg/day). All mice were daily treated by oral gavage for 7 days. Individual faecal pellets were collected at days 0, 4 and 8 as well as plasma at day 8 for SCFA profiling. Additionally, after the sacrifice on day 8, the caecum was weighted, and colon length was measured. The proximal colon was cut for histological analysis.

Results: MMF treatment induced around 10% weight loss at the end of the protocol associated with a significant decrease in caecum weight and a slight reduction in colon length. Histological analysis showed significant architectural changes in colon epithelium. Moreover, we observed an overall decrease in SCFA concentrations in faecal samples, especially regarding acetate (at day 8, control 1040.6 ± 278.161 μM versus MMF 384.7 ± 80.5 μM, $p < 0.01$) and propionate (at day 8, control 185.94 ± 51.96 μM versus MMF 44.07 ± 14.66 μM, $p < 0.001$), and in plasma samples for butyrate (at day 8, control 0.91 ± 0.1 μM versus MMF 0.46 ± 0.1 μM, $p < 0.01$).

Conclusions: These results are consistent with functional impairment of the gut microbiome linked with digestive or systemic defects during MMF treatment.

* Correspondence: roland.lawson@unilim.fr
[1]Univ. Limoges, Inserm U1248, IPPRITT, F-87000 Limoges, France
[2]Faculté de Pharmacie, Université de Limoges, 2 rue du Dr Marcland, 87025 Limoges, France

Jardou *et al. BMC Pharmacology and Toxicology*   (2021) 22:66

Page 2 of 9

Background

Mycophenolic acid (MPA) is one of the most widely used immunosuppressants in transplantation and for the treatment of some autoimmune diseases [1–3]. MPA, used as a prodrug (mycophenolate mofetil or MMF) or a salt (mycophenolate sodium), is a potent, selective, non-competitive and reversible inhibitor of inosine-5′-monophosphate dehydrogenase 2 (IMPDH2). IMPDH2 plays a key role in the de novo purine nucleotide synthesis, on which lymphocytes rely for DNA biosynthesis. Therefore, MPA exerts preferentially a cytostatic effect in T and B lymphocytes, which do not possess the recovery pathway for DNA biosynthesis through hypoxanthine-guanine phosphoribosyltransferase (HPRT) [4]. After oral absorption, MPA enters the systemic circulation where it directly acts on circulating lymphocytes. MPA can also reach lymphoid tissues (e.g., bone marrow, thymus, lymph nodes and spleen) for modulating in situ lymphocyte differentiation and activation [5, 6].

MPA treatment is unfortunately associated with adverse effects, among which gastrointestinal disorders are of major concern [7]. More than 30% of patients experience gastrointestinal adverse effects, ranging from nausea, vomiting, abdominal pain or diarrhoea, to erosions of the gastrointestinal tract with life-threatening bleeding ulcerations [8, 9]. Histologically, the lesions are characterized by architectural disorganization of the digestive epithelium mainly in the colon. Oedema and/or inflammation of the *lamina propria* are also observed, mimicking the inflammatory lesions of graft-versus-host disease in bone marrow transplantation [7, 10–12].

Recent investigations have pointed to the alteration of the gut microbiome, also referred to as intestinal dysbiosis, by immunosuppressive agents. Moreover, intestinal dysbiosis is responsible for abnormal gut microbiome β-glucuronidase activity and increased gastrointestinal exposure to MPA in mycophenolate-induced enteropathy [13–16]. MPA was first isolated as a fermentation product of *Penicillium stoloniferum* and was initially known for its antibacterial, antifungal, and antiviral properties [4]. Therefore, gastrointestinal tract exposure to high concentrations of MPA is expected to be associated with intestinal dysbiosis characterized by a decrease in density and diversity of the gut microbiome regarding the main bacterial phyla (e.g., Firmicutes and Bacteroidetes) which has been recently validated with a mouse model [15, 16]. These bacterial phyla are known for their metabolic role in maintaining the homeostasis of the digestive tract, particularly through the production of short-chain fatty acids (SCFA) from the fermentation of indigestible carbohydrates [17–20]. The three main SCFA (acetate, propionate and butyrate) can passively penetrate and pass through intestinal cells. SCFA can also be actively incorporated through sodium-coupled monocarboxylate transporter 1 (SMCT1) or monocarboxylate transporter 1 (MCT1) located on the apical side of intestinal epithelial cells and transported into the bloodstream through monocarboxylate transporter 4 and 5 (MCT4 and MCT5) found on the basolateral side [21–23]. SCFA are pharmacologically active and can selectively regulate three different G-protein coupled receptors (GPCR) on intestinal cells, namely, GPR41 (free fatty acid receptor 3 or FFAR3), GPR43 (free fatty acid receptor 2 or FFAR2) and GPR109A (hydroxycarboxylic acid receptor 2 or HCAR2) [24–26]. These receptors are also expressed on various other cell types in organs and tissues such as the liver, muscles, neurons and immune cells (T and B cells, macrophages) [27, 28]. SCFA function as "co-hormones" as they are produced by the gut microbiome, which is assimilated to a metabolic organ. Intracellular SCFA can exhibit a strong histone deacetylase (HDAC) inhibitory effect, with butyrate being the most potent inhibitor [29–32]. Histone hyperacetylation is associated with increased accessibility of promoter regions and genes modulation [33]. For example, butyrate through its HDAC inhibitory activity, can imprint an antimicrobial program in macrophages and thus, eliminate invasive pathogens and regulate the inflammatory response [34]. Butyrate can also be a source of energy for the colonocytes and can improve epithelial barrier functions through up-regulation of tight junctions proteins such as Claudin-1 and ZO-1 [35, 36]. SCFA may also have beneficial effects on gut homeostasis by enhancing mucosal barrier integrity through Mucin-2 expression [37]. Hence, the functional alterations of the SCFA profile can be involved in the pathophysiology of the mycophenolate-induced enteropathy. Our study aimed at analyzing the alterations of the SCFA profile at the local and systemic levels and their associations with the gastrointestinal toxicity of mycophenolic acid in a mouse model.

Methods

Experimental animals

In this study, our experimental model is inspired by the pioneering work published by Flannigan et al., 2018 [16] and Taylor et al., 2019 [15], which demonstrated an impairment of the gut microbial community associated with colon tissue inflammation under MPA treatment.

For this purpose, female C57BL/6 J adult (10 weeks old) Specific and Opportunistic Pathogen Free mice purchased from Janvier Labs (Saint-Berthevin, France) were used for in vivo experiments and were housed in a pathogen-free animal facility, with 12 h/12 h of light/dark and unrestricted access to food and water. The Regional Ethics Committee for Animal Experimentation (CEEA-033, Région Limousin) and the French Ministry of Higher Education, Research and Innovation, under Project Authorization for the use of Animals for Scientific Purposes 23,785-2,020,012,416,174,896 v3, approved animal care and experimental procedures. These experimental procedures were performed in accordance with the guidelines for animal experimentation of the European Communities Council Directive (EU/63/2010) and reported according to the ARRIVE guidelines [38]. Eighteen mice were randomly assigned into two groups: control (n = 9) and MMF (n = 9) and treated for 7 days. Mice were daily monitored for body weight. MMF treatment (900 mg/kg/day of a clinical formulation of MMF (Cellcept®) dissolved in saline solution) or saline solution (control group) were given by oral gavage with a 20 Gauge dosing cannula. For the sacrifice, the mice were anaesthetized with intraperitoneal injection of pentobarbital (100 mg/kg, CEVA Santé Animale, France).

Sample collection and storage
Faeces
Individual faecal pellets were collected using metabolic cages at day 0, day 4 and day 8 and were placed in a sterile collection tube and stored at − 80 °C for SCFA analysis.

Plasmas
Peripheral blood was obtained using a 22 Gauge heparinised syringe from anaesthetised mice on day 8 by intracardiac puncture and plasma was prepared by centrifugation at 10,000 g for 10 min at 4 °C and stored at − 80 °C for SCFA analysis.

Caecum/colon block
The block caecum/colon was harvested after sacrifice. The caecum was weighted and colon length measured. The proximal colon (around 1 cm) was cut and placed in a 4% formaldehyde solution for histological analysis.

SCFA quantification
Samples preparations
To quantify the SCFA in faecal samples, 25 μL of 50% aqueous acetonitrile solution was added to 1 mg of faeces, vortex mixed for 10 min and then placed for 10 min in an ultrasonic bath. The samples were centrifuged at 10,000 g at 10 °C for 10 min. The supernatants were collected. This procedure was repeated twice for each faecal sample and the supernatants were pooled. For plasma SCFA analysis, the samples were directly diluted 1:5 with a saline solution. Calibration standards (acetate from 10 to 5000 μM, propionate from 1 to 500 μM, butyrate from 0.4 to 200 μM) were prepared either in 50% aqueous acetonitrile for faecal samples or in saline solution for plasma samples.

The SCFA derivatization step was based on a previously published method [39]. Briefly, 50 μL of each sample (pooled supernatants for faeces or diluted plasma) were mixed with 20 μL of 200 mM 3-NPH, 20 μL of 120 mM EDC-6% pyridine, both solubilised in 50% aqueous acetonitrile solution, and 20 μL of pooled internal standard solution (D4-acetic acid 10 mM, D2-propionic acid 0.4 mM, D7-butyric acid 0.25 mM diluted in ultrapure water). The reaction was performed at 40 °C for 30 min in the dark and the samples were then diluted 1:20 (v/v) with 10% aqueous acetonitrile, and 1 μl or 5 μl thereof (for faeces or plasma derivation mixture respectively) were analysed by LC-MS/MS.

LC-MS/MS analysis
Briefly, chromatographic separation was performed using a Shimadzu Nexera 2 LC system (Shimadzu Corporation, Marne-la-Vallée, France) equipped with a thermostated column compartment and a thermostated microwell plate autosampler with a six-port microswitching valve. LC separation was performed on an Accucore™ RP-MS column (100 × 2.1 mm, 2.6 μm solid core, Thermo Scientific) at a flow rate of 0.2 mL/min at 60 °C. The mobile phase was a gradient of 0.1% formic acid in water (solvent A) and 0.1% formic acid in methanol (solvent B) programmed as follows: 0-0.5 min, 30% B; 0.5-8 min, 30 to 50% B; 8-9 min, 50 to 95% B; 9-11 min, 95% B; 11-11.5 min, 95 to 30% B; 11.5-15 min, 30% B. Detection was carried out with a LCMS8060 mass spectrometer (Shimadzu) in the positive ionization mode. Of the four optimized MRM transitions per analyte, the most intense and specific Q1/Q3 pair was selected for quantification: 194 > 137 for acetic acid, 197 > 137 for D4-acetate, 208 > 137 for propionic acid, 210 > 137 for D2-propionate, 222 > 137 for butyric acid and 229 > 137 for D7-butyrate. The MRM parameters for all analytes and their internal standards are listed in Table S1. The concentration of each SCFA was determined by calculating its corresponding peak area ratio to that of the IS using a linear regression with 1/x weighting to the calibration curve.

Histological analysis
Fixed proximal colon samples were paraffin-embedded, sectioned at 4 μm and stained with haematoxylin, eosin and saffron (HES). The slides were scanned using an automatic slide scanner (Nanozoomer, HAMAMATSU

PHOTONICS K.K., Systems Division, Japan) and images obtained were analysed using NDP.view2 (version 2.8, HAMAMATSU PHOTONICS K.K., Systems Division, Japan) and ImageJ (version 1.53) [40] software. The lesions were quantified based on variations of tissue interface, which are obtained by the difference between the whole section and the luminal section.

Statistical analysis
Statistical analysis of the data was performed using GraphPad Prism (version 5.00 for Windows, GraphPad Software, San Diego California USA, www.graphpad.com) and data are reported as arithmetic mean ± standard error of the mean (SEM). Statistical comparisons between experimental groups were performed using unpaired t-test or two-way ANOVA. A value of $p < 0.05$ was considered significant. When applied, the post-hoc test of Bonferroni was conducted if F value in ANOVA achieved statistical significance ($p < 0.05$) with no significant variance inhomogeneity. Partial least squares discriminant analysis (PLS-DA) score plots were made using the R Tidyverse package [41].
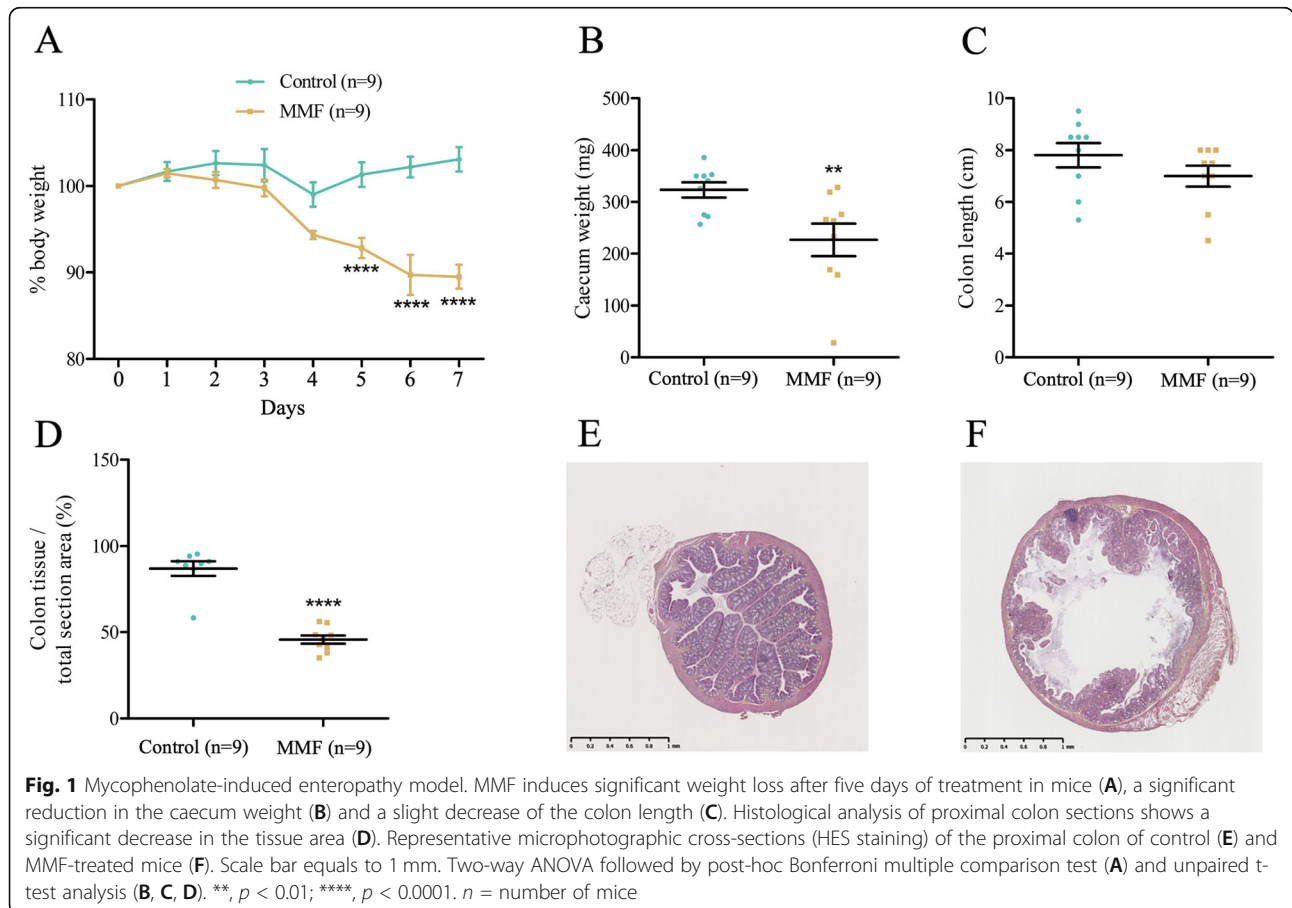
Results
MPA-induced enteropathy mouse model
MMF treatment is associated with a significant weight loss starting at day 5 to reach approximately 10% at day 7 (control 103.1 ± 1.41% versus MMF 89.88 ± 1.28%, $p < 0.0001$) (Fig. 1A). This body weight loss is accompanied by a significant reduction in caecum weight (control 323.3 ± 14.87 mg versus MMF 226.8 ± 31.51 mg, $p < 0.01$) (Fig. 1B) and a slight, non-significant decrease in colon length (control 7.81 ± 0.47 cm versus MMF 7.00 ± 0.41 cm, $p > 0.05$) (Fig. 1C). Histological analysis revealed overall architectural disorganization and a significant decrease in the proximal colon tissue area (control 86.94 ± 4.21% versus MMF 45.68 ± 2.42%, $p < 0.0001$) (Fig. 1D). Microphotographic observations showed an almost complete destruction of the intestinal crypts and villi in MMF-treated mice in comparison to controls (Fig. 1E and F). Altogether, these data corroborate the development of a validated model of gastrointestinal toxicity in mice.

SCFA profile alterations
Modifications in the digestive production of SCFA
SCFA in faeces were quantified at days 0, 4 and 8 to investigate functional alterations of the gut microbiome

Fig. 1 Mycophenolate-induced enteropathy model. MMF induces significant weight loss after five days of treatment in mice (**A**), a significant reduction in the caecum weight (**B**) and a slight decrease of the colon length (**C**). Histological analysis of proximal colon sections shows a significant decrease in the tissue area (**D**). Representative microphotographic cross-sections (HES staining) of the proximal colon of control (**E**) and MMF-treated mice (**F**). Scale bar equals to 1 mm. Two-way ANOVA followed by post-hoc Bonferroni multiple comparison test (**A**) and unpaired t-test analysis (**B**, **C**, **D**). **, $p < 0.01$; ****, $p < 0.0001$. n = number of mice
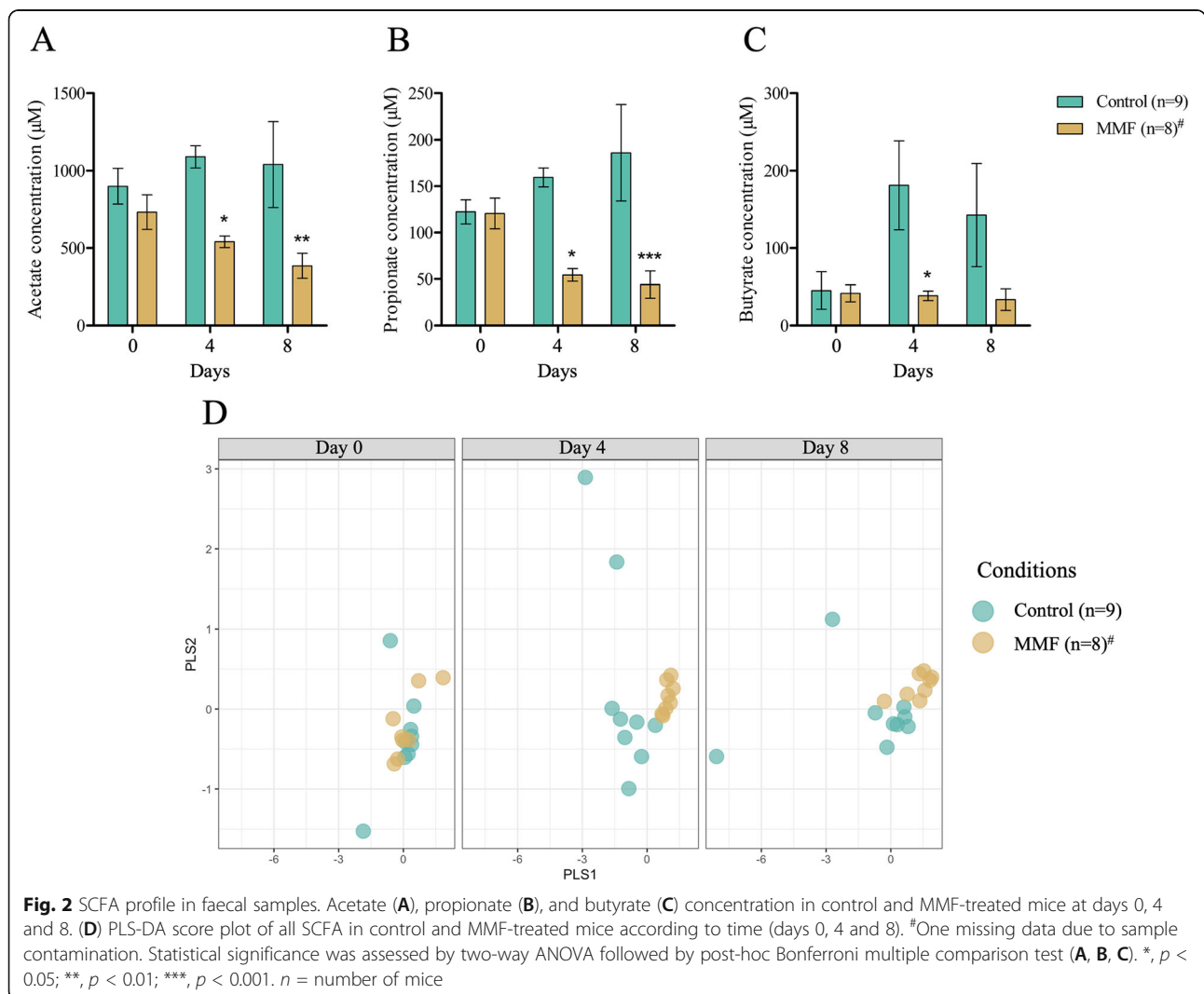
induced by MMF. We found a significant decrease of acetate at day 4 (control 1090.5 ± 71.88 µM versus MMF 540.3 ± 37.6 µM, $p < 0.05$) and day 8 (control 1040.6 ± 278.161 µM versus MMF 384.7 ± 80.5 µM, $p < 0.01$) in MMF-treated mice in comparison to controls (Fig. 2A). The results was similar for propionate concentrations at day 4 (control 159.5 ± 10.27 µM versus MMF 54.34 ± 6.84 µM, $p < 0.05$) and day 8 (control 185.94 ± 51.96 µM versus MMF 44.07 ± 14.66 µM, $p < 0.001$) (Fig. 2B). Overall, there was no time-dependent modification in butyrate concentrations for MMF-treated mice despite fluctuation in the control group, leading to a significant difference only at day 4 (control 181.1 ± 57.4 µM versus MMF 38.55 ± 6.08 µM, $p < 0.05$) (Fig. 2C). The score plot of the PLS-DA model which includes concentrations of the three SCFA (acetate, propionate, butyrate) showed two groups at days 4 and 8 (Fig. 2D).
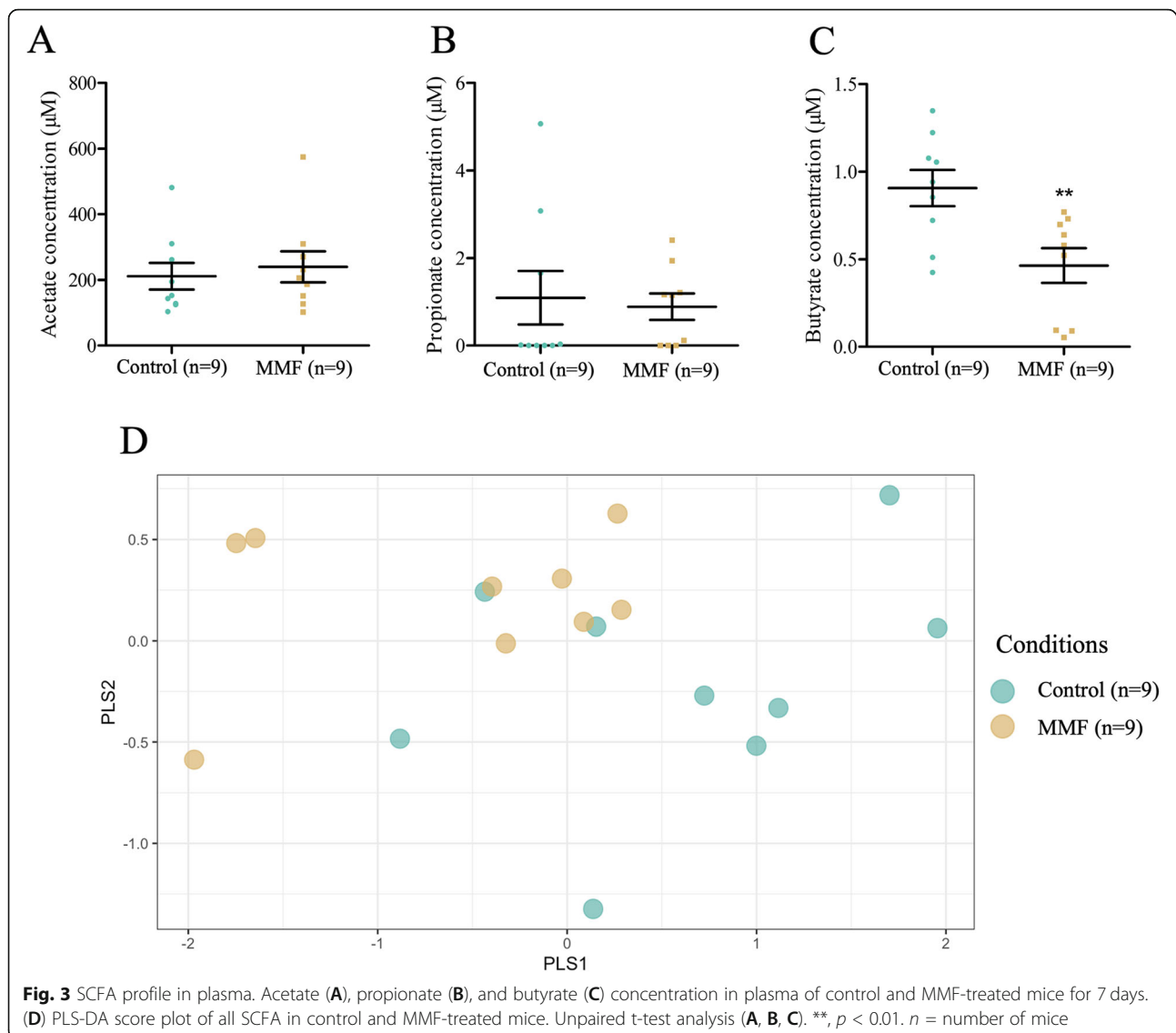
Modifications of SCFA plasma concentrations
SCFA in plasma were quantified from samples obtained at day 8 after sacrifice. There was no change in acetate (control 211.5 ± 40.76 µM versus MMF 240.2 ± 47.41 µM, $p > 0.05$) or propionate (control 1.09 ± 0.61 µM versus MMF 0.89 ± 0.3 µM, $p > 0.05$) concentrations (Fig. 3A and B). In contrast, a significant decrease in butyrate concentrations was observed (control 0.91 ± 0.1 µM versus MMF 0.46 ± 0.1 µM, $p < 0.01$) (Fig. 3C). Again, the score plot of the PLS-DA model with the three SCFA showed two groups (Fig. 3D).

Discussion
In the current study, we developed and validated a mouse model of mycophenolate-induced enteropathy that showed typical remodelling lesions of the colonic epithelium architecture. Detailed analyses of the concentration-time profile of the three main SCFA

Fig. 2 SCFA profile in faecal samples. Acetate (**A**), propionate (**B**), and butyrate (**C**) concentration in control and MMF-treated mice at days 0, 4 and 8. (**D**) PLS-DA score plot of all SCFA in control and MMF-treated mice according to time (days 0, 4 and 8). [#]One missing data due to sample contamination. Statistical significance was assessed by two-way ANOVA followed by post-hoc Bonferroni multiple comparison test (**A**, **B**, **C**). *, $p < 0.05$; **, $p < 0.01$; ***, $p < 0.001$. n = number of mice

Fig. 3 SCFA profile in plasma. Acetate (**A**), propionate (**B**), and butyrate (**C**) concentration in plasma of control and MMF-treated mice for 7 days. (**D**) PLS-DA score plot of all SCFA in control and MMF-treated mice. Unpaired t-test analysis (**A**, **B**, **C**). **, $p < 0.01$. n = number of mice

revealed for the first time a functional alteration of the gut microbiome associated with MPA.

Severe enteropathy associated with MPA treatment
Our mice present an important decrease in body weight and exhibit typical and severe histological lesions, characterized by oedematous colonic mucosa with withering or marked crypt drop-out and villi destructions. These observations are consistent with the pattern of inflammatory injuries observed in treated patients with endoscopic evidence of ulcers and erosions [10–12]. Histologically, in these patients, the pattern of injury is typified by prominent crypt apoptosis with graft-versus-host-like-disease [8, 42, 43]. The caecum weight and colon length reduction could result from the direct impact of MPA on intestinal cells homeostasis [44].

Alterations of the gut microbiome in mycophenolate-induced enteropathy
Recent reports have highlighted intestinal dysbiosis associated with MPA therapy [15, 16]. Intestinal dysbiosis has been linked to the decrease of the main pro-resolving mediators involved in the control of inflammatory processes and tissue damage [45, 46]. Our investigations thereby focus on the SCFA concentration-time profile and demonstrate digestive and systemic alterations in mycophenolate-induced enteropathy in mice. Indeed, there is a drastic reduction in digestive SCFA production of acetate and propionate that could contribute to the pathophysiology of mycophenolate-induced enteropathy. Along with this, it has been shown that germ-free or large spectrum antibiotic-treated mice show reduced proliferative activity of intestinal epithelial cells, which is reversed by SCFA supplementation [47].

Moreover, acetate, propionate and butyrate promote the development of intestinal organoids in vitro [47, 48]. In addition, increased gut microbiota SCFA production had a protective effect on a mouse model of acute experimental colitis [49, 50]. SCFA also diminished the development of tumours and attenuated colonic inflammation in a mouse model of colitis-associated colorectal cancer [51]. SCFA exert important roles in gut homeostasis and might be proposed as supportive therapy for patients treated with MPA.

Our data also demonstrate an important reduction of systemic plasma butyrate concentrations that might initiate pathological pathways in patients. Indeed, a close link between butyrate decrease and the onset of some cardiovascular or metabolic events was described [52]. For instance, de novo diabetes after solid organ transplantation is a complication that increases the risk of infections and graft failure in liver or kidney transplant patients [53, 54]. The immunosuppressive regimen also plays a critical role in the development of de novo diabetes, since tacrolimus and MMF strongly increase the incidence of new-onset diabetes after liver transplantation [55]. Butyrate supplementation promotes the mitigation of insulin resistance in animal models and protects against metabolic disorders [56, 57]. Regarding cardiovascular co-morbidities, arterial hypertension is frequently observed in kidney transplant patients [58]. Again, butyrate might exert a protective role since it suppressed angiotensin II-induced hypertension in a rat model [59].

Further investigations are needed to study the link between specific chronic diseases that require transplantation and the worsening of SCFA profile in post-transplantation periods. Moreover, the alterations of the gut microbiome induced by MPA could rationalize the progressive growth in the incidence of multidrug-resistance and extensively-drug-resistant strains in transplant patients [60, 61].

This will be helpful to decipher the specific impact of immunosuppressants. SCFA profile could be used as either as a predictive or a diagnostic biomarker for the follow-up of transplanted patients. SCFA supplementation might also be beneficial for treating mycophenolate-induced enteropathy.

Conclusions

Our investigations reveal for the first time alterations of the SCFA time-profile in a mouse model of mycophenolate-induced enteropathy. This alteration could locally contribute to the inflammatory processes of mycophenolate-induced enteropathy. Moreover, decreased butyrate plasma concentrations might trigger pathological pathways leading to cardiovascular or metabolic comorbidities such as arterial hypertension or de novo diabetes in MPA-treated patients. Further investigations are needed to establish the molecular mechanisms and their relevance in human pathology. If these hypotheses are confirmed, SCFA can be envisaged in supplementation to improve the patients' quality of life or as biomarkers of mycophenolate-induced enteropathy.

Abbreviations
(S)MCT: (Sodium-coupled) monocarboxylate transporter; 3-NPH: 3-nitrophenylhydrazine; EDC: N-(3-dimethylaminopropyl)-N′-ethylcarbodiimide; FFAR: Free fatty acid receptor; GPCR: G-protein coupled receptors; HDAC: Histone deacetylase; HES: Haematoxylin, eosin and saffron; HPRT: Hypoxanthine-guanine phosphoribosyltransferase; IMPDH2: Inosine-5′-monophosphate dehydrogenase 2; MMF: Mycophenolic mofetil; MPA: Mycophenolic acid; PLS-DA: Partial least squares discriminant analysis; SCFA: Short-chain fatty acid

Supplementary Information

The online version contains supplementary material available at https://doi.org/10.1186/s40360-021-00536-4.

Additional file 1.

Authors' contributions
M.J, E. P, and R. L designed the study, were involved in planning, and supervised the work. M. J and R. L performed analysis, drafted the manuscript, and designed the Figs. Q. P and C. B performed experiments supervised by M. J, E. P and R.L. E. P and F-L.S developed techniques of mass spectrometry. M. J and R. L wrote the paper with input from all authors, who have read and approved the final manuscript.

Availability of data and materials
The datasets used and/or analysed during this study are available from the corresponding author on reasonable request.

Declarations

Ethics approval and consent to participate
The Regional Ethics Committee for Animal Experimentation (CEEA-033, Région Limousin) and the French Ministry of Higher Education, Research and Innovation, under Project Authorization for the use of Animals for Scientific Purposes 23785-2020012416174896 v3, approved animal care and experimental procedures. These experimental procedures were performed in accordance with the guidelines for animal experimentation of the European Communities Council Directive (EU/63/2010).

Consent for publication
Not applicable.

Competing interests
There are no competing interests to declare.

Jardou *et al. BMC Pharmacology and Toxicology*   (2021) 22:66

Page 8 of 9

References

1. Allison AC. Mechanisms of action of mycophenolate mofetil in preventing chronic rejection. Transplant Proc. 2002;34(7):2863–6.
2. Srinivas TR, Kaplan B, Meier-Kriesche H-U. Mycophenolate mofetil in solid-organ transplantation. Expert Opin Pharmacother. 2005;4(12):2325–45.
3. Zizzo G, De Santis M, Ferraccioli GF. Mycophenolic acid in rheumatology: mechanisms of action and severe adverse events. Reumatismo. 2010;62(2):91–100.
4. Allison AC, Eugui EM. Mycophenolate mofetil and its mechanisms of action. Immunopharmacology. 2000;47(2–3):85–118.
5. Ferjani H, Draz H, Abid S, Achour A, Bacha H, Boussema-Ayed I. Combination of tacrolimus and mycophenolate mofetil induces oxidative stress and genotoxicity in spleen and bone marrow of Wistar rats. Mutat Res Toxicol Environ Mutagen. 2016;810:48–55.
6. Eugui EM, Mirkovich A, Allison AC. Lymphocyte-selective Antiproliferative and immunosuppressive effects of mycophenolic acid in mice. Scand J Immunol. 1991;33(2):175–83.
7. Kitchin JES, Pomeranz MK, Pak G, Washenik K, Shupack JL. Rediscovering mycophenolic acid: a review of its mechanism, side effects, and potential uses. J Am Acad Dermatol. 1997;37(3):445–9.
8. Al-Absi AI, Cooke CR, Wall BM, Sylvestre P, Ismail MK, Mya M. Patterns of injury in mycophenolate Mofetil–related colitis. Transplant Proc. 2010;42(9):3591–3.
9. Behrend M. Adverse gastrointestinal effects of mycophenolate Mofetil. Drug Saf. 2001;24(9):645–63.
10. Seminerio J, McGrath K, Arnold CA, Voltaggio L, Singhi AD. Medication-associated lesions of the GI tract. Gastrointest Endosc. 2014;79(1):140–50.
11. Calmet FH, Yarur AJ, Pukazhendhi G, Ahmad J, Bhamidimarri KR. Endoscopic and histological features of mycophenolate mofetil colitis in patients after solid organ transplantation. Ann Gastroenterol Q Publ Hell Soc Gastroenterol. 2015;28(3):366.
12. Selbst MK, Ahrens WA, Robert ME, Friedman A, Proctor DD, Jain D. Spectrum of histologic changes in colonic biopsies in patients treated with mycophenolate mofetil. Mod Pathol. 2009;22(6):737–43.
13. Tourret J, Willing BP, Dion S, MacPherson J, Denamur E, Finlay BB. Immunosuppressive treatment alters secretion of ileal antimicrobial peptides and gut microbiota, and favors subsequent colonization by uropathogenic Escherichia coli. Transplantation. 2017;101(1):74–82.
14. Gibson CM, Childs-Kean LM, Naziruddin Z, Howell CK. The alteration of the gut microbiome by immunosuppressive agents used in solid organ transplantation. Transpl Infect Dis. 2021;23:e13397.
15. Taylor MR, Flannigan KL, Rahim H, Mohamud A, Lewis IA, Hirota SA, et al. Vancomycin relieves mycophenolate mofetil–induced gastrointestinal toxicity by eliminating gut bacterial β-glucuronidase activity. Sci Adv. 2019;5(8):eaax2358.
16. Flannigan KL, Taylor MR, Pereira SK, Rodriguez-Arguello J, Moffat AW, Alston L, et al. An intact microbiota is required for the gastrointestinal toxicity of the immunosuppressant mycophenolate mofetil. J Heart Lung Transplant. 2018;37(9):1047–59.
17. Parada Venegas D, De la Fuente MK, Landskron G, González MJ, Quera R, Dijkstra G, et al. Short chain fatty acids (SCFAs)-mediated gut epithelial and immune regulation and its relevance for inflammatory bowel diseases. Front Immunol. 2019;10:277.
18. Tsukuda N, Yahagi K, Hara T, Watanabe Y, Matsumoto H, Mori H, et al. Key bacterial taxa and metabolic pathways affecting gut short-chain fatty acid profiles in early life. ISME J. 2021;15:1–17.
19. Reichardt N, Duncan SH, Young P, Belenguer A, McWilliam Leitch C, Scott KP, et al. Phylogenetic distribution of three pathways for propionate production within the human gut microbiota. ISME J. 2014;8(6):1323–35.
20. Zhang Z, Tang H, Chen P, Xie H, Tao Y. Demystifying the manipulation of host immunity, metabolism, and extraintestinal tumors by the gut microbiome. Signal Transduct Target Ther. 2019;4(1):1–34.
21. Cuff MA, Lambert DW, Shirazi-Beechey SP. Substrate-induced regulation of the human colonic monocarboxylate transporter, MCT1. J Physiol. 2002;539(Pt 2):361.
22. Miyauchi S, Gopal E, Fei Y-J, Ganapathy V. Functional identification of SLC5A8, a tumor suppressor Down-regulated in Colon Cancer, as a Na+

–coupled transporter for short-chain fatty acids. J Biol Chem. 2004;279(14):13293–6.
23. Gill RK, Saksena S, Alrefai WA, Sarwar Z, Goldstein JL, Carroll RE, et al. Expression and membrane localization of MCT isoforms along the length of the human intestine. Am J Phys Cell Phys. 2005;289:846–52.
24. Brown AJ, Goldsworthy SM, Barnes AA, Eilert MM, Tcheang L, Daniels D, et al. The orphan G protein-coupled receptors GPR41 and GPR43 are activated by propionate and other short chain carboxylic acids. J Biol Chem. 2003;278(13):11312–9.
25. Zhao Y, Chen F, Wu W, Sun M, Bilotta AJ, Yao S, et al. GPR43 mediates microbiota metabolite SCFA regulation of antimicrobial peptide expression in intestinal epithelial cells via activation of mTOR and STAT3. Mucosal Immunol. 2018;11(3):752–62.
26. Thangaraju M, Cresci GA, Liu K, Ananth S, Gnanaprakasam JP, Browning DD, et al. GPR109A is a G-protein-coupled receptor for the bacterial fermentation product butyrate and functions as a tumor suppressor in colon. Cancer Res. 2009;69(7):2826.
27. Le Poul E, Loison C, Struyf S, Springael JY, Lannoy V, Decobecq ME, et al. Functional characterization of human receptors for short chain fatty acids and their role in Polymorphonuclear cell activation. J Biol Chem. 2003;278(28):25481–9.
28. Van Der Hee B, Wells JM. Microbial regulation of host physiology by short-chain fatty acids. Trends Microbiol. 2021;29:700–12.
29. Rada-Iglesias A, Enroth S, Ameur A, Koch CM, Clelland GK, Respuela-Alonso P, et al. Butyrate mediates decrease of histone acetylation centered on transcription start sites and down-regulation of associated genes. Genome Res. 2007;17(6):708.
30. Basson MD, Liu YW, Hanly AM, Emenaker NJ, Shenoy SG, Rothberg BEG. Identification and comparative analysis of human colonocyte short-chain fatty acid response genes. J Gastrointest Surg. 2000;4(5):501–12.
31. Candido EPM, Reeves R, Davie JR. Sodium butyrate inhibits histone deacetylation in cultured cells. Cell. 1978;14(1):105–13.
32. Sealy L, Chalkley R. The effect of sodium butyrate on histone modification. Cell. 1978;14(1):115–21.
33. Xu WS, Parmigiani RB, Marks PA. Histone deacetylase inhibitors: molecular mechanisms of action. Oncogene. 2007;26(37):5541–52.
34. Schulthess J, Pandey S, Capitani M. The Short Chain Fatty Acid Butyrate Imprints an Antimicrobial Program in Macrophages. Immunity. 2019;50:432–445.e7.
35. Donohoe DR, Garge N, Zhang X, Sun W, O'Connell TM, Bunger MK, et al. The microbiome and butyrate regulate energy metabolism and autophagy in the mammalian Colon. Cell Metab. 2011;13(5):517–26.
36. Wang HB, Wang PY, Wang X, Wan YL, Liu YC. Butyrate enhances intestinal epithelial barrier function via up-regulation of tight junction protein claudin-1 transcription. Dig Dis Sci. 2012;57(12):3126–35.
37. Willemsen LEM, Koetsier MA, van Deventer SJH, van Tol EAF. Short chain fatty acids stimulate epithelial mucin 2 expression through differential effects on prostaglandin E1 and E2 production by intestinal myofibroblasts. Gut. 2003;52(10):1442.
38. Lilley E, Stanford SC, Kendall DE, Alexander SPH, Cirino G, Docherty JR, et al. ARRIVE 2.0 and the British Journal of pharmacology: updated guidance for 2020. Br J Pharmacol. 2020;177(16):3611–6.
39. Han J, Lin K, Sequeira C, Borchers CH. An isotope-labeled chemical derivatization method for the quantitation of short-chain fatty acids in human feces by liquid chromatography–tandem mass spectrometry. Anal Chim Acta. 2015;854:86–94.
40. Schneider CA, Rasband WS, Eliceiri KW. NIH image to ImageJ: 25 years of image analysis. Nat Methods. 2012;9(7):671–5.
41. Wickham H, Averick M, Bryan J, Chang W, McGowan LD, François R, et al. Welcome to the Tidyverse. J Open Source Softw. 2019;4(43):1686.
42. Papadimitriou JC, Cangro CB, Lustberg A, Khaled A, Nogueira J, Wiland A, et al. Histologic features of mycophenolate Mofetil-related colitis: a graft-versus-host disease-like pattern. Int J Surg Pathol. 2003;11(4):295–302.
43. Liapis G, Boletis J, Skalioti C, Bamias G, Tsimaratou K, Patsouris E, et al. Histological spectrum of mycophenolate mofetil-related colitis: association with apoptosis. Histopathology. 2013;63(5):649–58.
44. Heischmann S, Dzieciatkowska M, Hansen K, Leibfritz D, Christians U. The Immunosuppressant Mycophenolic Acid Alters Nucleotide and Lipid Metabolism in an Intestinal Cell Model. Sci Rep. 2017;7:45088.
45. Morgan XC, Tickle TL, Sokol H, Gevers D, Devaney KL, Ward DV, et al. Dysfunction of the intestinal microbiome in inflammatory bowel disease and treatment. Genome Biol. 2012;13(9):1–18.

46. Frank DN, Amand ALS, Feldman RA, Boedeker EC, Harpaz N, Pace NR. Molecular-phylogenetic characterization of microbial community imbalances in human inflammatory bowel diseases. Proc Natl Acad Sci U S A. 2007;104(34):13780.

47. Park J, Kotani T, Konno T, Setiawan J, Kitamura Y, Imada S, et al. Promotion of intestinal epithelial cell turnover by commensal Bacteria: role of short-chain fatty acids. PLoS One. 2016;11(5):e0156334.

48. Lukovac S, Belzer C, Pellis L, Keijser BJ, de Vos WM, Montijn RC, et al. Differential modulation by Akkermansia muciniphila and Faecalibacterium prausnitzii of host peripheral lipid metabolism and histone acetylation in mouse gut organoids. MBio. 2014;5:e01438–14.

49. Tan B, Luo W, Shen Z, Xiao M, Wu S, Meng X, et al. Roseburia intestinalis inhibits oncostatin M and maintains tight junction integrity in a murine model of acute experimental colitis. Scand J Gastroenterol. 2019;54(4):432–40.

50. Ji J, Shu D, Zheng M, Wang J, Luo C, Wang Y, et al. Microbial metabolite butyrate facilitates M2 macrophage polarization and function. Sci Rep. 2016; 6:24838.

51. Tian Y, Xu Q, Sun L, Ye Y, Ji G. Short-chain fatty acids administration is protective in colitis-associated colorectal cancer development. J Nutr Biochem. 2018;57:103–9.

52. Bik EM, Ugalde JA, Cousins J, Goddard AD, Richman J, Apte ZS. Microbial biotransformations in the human distal gut. Br J Pharmacol. 2018;175(24): 4404–14.

53. Washer GF, Schröter GPJ, Starzl TE, Iii RW. Causes of death after kidney transplantation. JAMA. 1983;250(1):49–54.

54. Stepanova M, Henry L, Garg R, Kalwaney S, Saab S, Younossi Z. Risk of de novo post-transplant type 2 diabetes in patients undergoing liver transplant for non-alcoholic steatohepatitis. BMC Gastroenterol. 2015;15:175.

55. Liu F-C, Lin H-T, Lin J-R, Yu H-P. Impact of immunosuppressant therapy on new-onset diabetes in liver transplant recipients. Ther Clin Risk Manag. 2017; 13:1043–51.

56. Gao Z, Yin J, Zhang J, Ward RE, Martin RJ, Lefevre M, et al. Butyrate improves insulin sensitivity and increases energy expenditure in mice. Diabetes. 2009;58(7):1509.

57. Zhang L, Du J, Yano N, Wang H, Zhao YT, Patricia D-S, et al. Sodium butyrate protects against high fat diet-induced cardiac dysfunction and metabolic disorders in type II diabetic mice HHS public access. J Cell Biochem. 2017;118(8):2395–408.

58. Severova-Andreevska G, Danilovska I, Sikole A, Popov Z, Ivanovski N. Hypertension after kidney transplantation: clinical significance and Therapeutical aspects. Open Access Maced J Med Sci. 2019;7(7):1241.

59. Wang L, Zhu Q, Lu A, Liu X, Zhang L, Xu C, et al. Sodium butyrate suppresses angiotensin II-induced hypertension by inhibition of renal (pro) renin receptor and intrarenal renin-angiotensin system. J Hypertens. 2017; 35(9):1899–908.

60. Cervera C, van Delden C, Gavaldà J, Welte T, Akova M, Carratalà J. Multidrug-resistant bacteria in solid organ transplant recipients. Clin Microbiol Infect. 2014;20(s7):49–73.

61. Jin M, Zeng L, Zhang W, Deng X, Li J, Zhang W. Clinical features of multidrug-resistant organism infections in early postoperative solid organ transplantation in a single center. Ann Palliat Med. 2021;10(4):4555562–4562.

Publisher's Note